Title: Temperature determines Zika, dengue and chikungunya transmission potential in the Americas

Authors: Erin A. Mordecai[a*], Jeremy M. Cohen[b], Michelle V. Evans[c], Prithvi Gudapati[a], Leah R. Johnson[b], Kerri Miazgowicz[d], Courtney C. Murdock[c,d], Jason R. Rohr[b], Sadie J. Ryan[e,f,g,h], Van Savage[i,j], Marta Shocket[k], Anna Stewart Ibarra[l], Matthew B. Thomas[m], Daniel P. Weikel[n]

Affiliations:

[a]Biology Department, Stanford University, 371 Serra Mall, Stanford, CA 94305

[b]Department of Integrative Biology, University of South Florida, 4202 East Fowler Ave, SCA110 Tampa, FL 33620

[c]Odum School of Ecology, University of Georgia, 140 E. Green St., Athens, GA 30602

[d]Center for Tropical and Emerging Global Disease, Department of Infectious Diseases, University of Georgia College of Veterinary Medicine, 501 D.W. Brooks Drive, Athens, GA 30602

[e]Department of Geography, University of Florida, PO Box 117315, Turlington Hall, Gainesville, FL 32611

[f]Emerging Pathogens Institute, University of Florida, P.O. Box 100009, 2055 Mowry Road Gainesville, FL 32610

[g]Center for Global Health and Translational Science, Department of Microbiology and Immunology, Weiskotten Hall, SUNY Upstate Medical University, Syracuse, NY 13210

[h]School of Life Sciences, College of Agriculture, Engineering, and Science, University of KwaZulu Natal, Private Bag X01, Scottsville, 3209, KwaZulu Natal, South Africa

[i]Department of Ecology and Evolutionary Biology, University of California Los Angeles and Department of Biomathematics, University of California Los Angeles, Los Angeles, CA 90095

[j]Santa Fe Institute, 1399 Hyde Park Rd, Santa Fe, NM 87501

[k]Department of Biology, Indiana University, 1001 E. 3rd St., Jordan Hall 142, Bloomington, IN 47405

[l]Center for Global Health and Translational Sciences, SUNY Upstate Medical University, Syracuse, NY13210

[m]Department of Entomology and Center for Infectious Disease Dynamics, Penn State University, 112 Merkle Lab, University Park, PA 16802

[n]Department of Biostatistics, University of Michigan, 1415 Washington Heights, Ann Arbor, MI 48109

[*]Correspondence to: Erin Mordecai. Biology Department, Stanford University, 371 Serra Mall, Stanford, CA 94305. (650) 497-7447. emordeca@stanford.edu

Classification: BIOLOGICAL SCIENCES: Ecology

Keywords: Zika, dengue, chikungunya, temperature, vector transmission, *Aedes aegypti*, *Aedes albopictus*

Abstract

Recent epidemics of Zika, dengue, and chikungunya have heightened the need to understand virus transmission ecology for *Aedes aegypti* and *Ae. albopictus* mosquitoes. An estimated 3.9 billion people in 120 countries are at risk for these diseases. Temperature defines the fundamental potential for vector-borne disease transmission, yet the potential for transmission in sub-tropical and temperate regions remains uncertain. Using mechanistic transmission models fit to mosquito and virus physiology data and validated with human case data, we show that mean temperature accurately bounds transmission risk for Zika, chikungunya, and dengue in the Americas. Transmission occurs between 18-34°C and peaks at 29°C for *Ae. aegypti* (between 11-28°C with a peak at 26°C for *Ae. albopictus*). As predicted, high relative incidence of Zika, dengue, and chikungunya in humans occurs between 23-32°C, peaks at 27-29°C, and is very low outside the predicted range. As a proxy for infrastructure and vector control effort, economic reliance on tourism explains some departures from areas otherwise suitable for high rates of transmission. Nonetheless, the temperature-based models alone provide fundamental eco-physiological measures of transmission potential. Tropical and subtropical regions are suitable for extended seasonal or year-round transmission by *Ae. aegypti* and *Ae. albopictus*. By contrast, potential transmission in temperate areas is constrained to at most three months per year even if vectors are present (which is currently not the case for large parts of the US). Such brief transmission windows limit the likelihood and potential extent of epidemics following disease introduction in temperate zones.

Significance statement

Viruses transmitted by *Aedes aegypti* and *Ae. albopictus* mosquitoes, including Zika, dengue, and chikungunya, present one of the most rapidly growing infectious disease threats, putting an

63 estimated 3.9 billion people in 120 countries at risk. Understanding the relationship between
64 transmission and climate, particularly temperature, is critical for predicting and responding to
65 potential spread into sub-tropical and temperate areas. Using models informed by laboratory
66 experiments and tested against actual human infection data, we show that transmission potential
67 of these three viruses is substantial between 23-32°C and peaks at 27-29°C. This implies that
68 while year-round transmission is likely in tropical and sub-tropical areas, temperate areas are at
69 risk for at most seasonal transmission, given that the necessary mosquito species are present.
70

Introduction

Epidemics of dengue, chikungunya, and Zika are sweeping through the Americas, part of a public health crisis that places an estimated 3.9 billion people in 120 countries at risk globally (1). Dengue virus (DENV) distribution and intensity in the Americas has increased over the last three decades, infecting an estimated 390 million people (96 million clinical) per year (2). Chikungunya virus (CHIKV) emerged in the Americas in 2013, causing 1.8 million suspected cases from 44 countries and territories (www.paho.org). In the last year, Zika virus (ZIKV) has spread throughout the Americas, causing nearly 500,000 suspected and confirmed cases, with many more unreported (http://ais.paho.org/phip/viz/ed_zika_cases.asp, as of July 7, 2016). The growing burden of these diseases (including links between Zika infection and microcephaly and Guillain-Barré syndrome (3)) and potential for spread into new areas creates an urgent need for predictive models that can inform risk assessment and guide interventions such as mosquito control, community outreach, and education.

Aedes aegypti, a mosquito with a close affiliation with and preference for humans, is the main vector of DENV, CHIKV, and ZIKV, while *Ae. albopictus*, a peri-urban mosquito, is an important secondary vector (4, 5). Predicting transmission of these viruses requires understanding the ecology of the vector species. Mathematical and geostatistical models that incorporate climate information have been immensely valuable for predicting and responding to *Aedes* spp. spread and DENV, CHIKV, and ZIKV outbreaks (5–9). Yet we currently lack a validated mechanistic model of the relationship between key climatic factors and transmission for *Ae. aegypti, Ae. albopictus*, and the arboviruses they transmit. We expect the role of climate, particularly temperature, to be predictable from fundamental ecological responses of mosquitoes and viruses to environmental conditions. Survival, feeding, development, and reproductive rates

94 predictably respond to temperature across a variety of ectotherms, including mosquitoes (10, 11).
95 Because these traits determine transmission rates, the effects of temperature on transmission
96 should also be broadly predictable from mechanistic models that incorporate temperature-
97 dependent traits.

98 Here, we synthesize available data to characterize the temperature-dependent traits of the
99 mosquitoes and viruses that determine transmission intensity. With these thermal responses, we
100 develop mechanistic temperature-dependent virus transmission models for *Ae. aegypti* and *Ae.*
101 *albopictus*, and validate them with DENV, CHIKV, and ZIKV human incidence data from the
102 Americas from 2014-2016. Because the relationship between transmission and incidence is
103 nonlinear, we better approximated transmission by dividing incidence by the cumulative number
104 of cases. We confined our analyses to the increasing portion of each epidemic, before susceptible
105 individuals become limiting and when transmission is most dependent on environmental
106 conditions. In validating the temperature-dependent mechanistic models, we examine the rates of
107 false positive and false negative predictions. If temperature fundamentally limits transmission
108 potential, high transmission should only occur under temperatures predicted to be highly
109 suitable, and areas with low predicted suitability should have low transmission (i.e., false
110 negative rates should be low). By contrast, low transmission may occur even when temperature
111 suitability is high because other factors like vector control can limit transmission (i.e., the false
112 positive rate should be higher than the false negative rate).

113 **Results**

114 Data gathered from the literature (9, 12–23) revealed that all mosquito traits relevant to
115 transmission peak between 23°C and 34°C for the two mosquito species (Figs. S1-S2). Humidity
116 linearly increases survival at all mosquito life stages, but does not interact with temperature (Fig.

S3). DENV extrinsic incubation and vector competence peak at 35°C (24–27) and 31-32°C (24, 25, 27, 28), respectively, in both mosquitoes—temperatures at which mosquito survival is low, limiting transmission potential (Figs. S1-S2). The parameterized models predict optimal transmission at 29°C by *Ae. aegypti* and 26°C by *Ae. albopictus* (Fig. 1). Transmission potential is zero below 14-18°C or above 34-35°C for *Ae. aegypti*, and below 11-16°C or above 28-32°C for *Ae. albopictus* (ranges depend on the amount of daily temperature variation; Figs. 1, S4-S5).

Weekly relative incidence of DENV, CHIKV, and ZIKV across countries in the Americas and the Caribbean is consistent with mechanistic model predictions (Fig. 1). The highest observed incidence occurs at 27°C for CHIKV and DENV and at 29°C for ZIKV, and the majority of transmission occurs between 23-32°C (i.e., false negative rate was low; Fig. 1). At a local scale, DENV relative incidence reported across 14 years in Iquitos, Peru and 24 years in San Juan, Puerto Rico also matches the predicted thermal optimum (Fig. S6). The accuracy of the model in bounding transmission potential is notable given the coarse scale of the human incidence versus mean temperature data (i.e., country-scale means for the DENV and CHIKV), the lack of CHIKV- and ZIKV-specific trait thermal response data to inform the model, the nonlinear relationship between transmission and incidence, and all the well-documented factors other than temperature that influence transmission. Together, these analyses show that temperature suitability for transmission is predictable from simple mechanistic models parameterized with laboratory data on the two mosquito species and dengue virus. Moreover, the similar responses of human incidence of ZIKV, CHIKV, and DENV to temperature suggest that the thermal ecology of their shared mosquito vectors is a key determinant of outbreak location, timing, and size.

High transmission only occurred where predicted by the model (Fig. 1) but as expected, some sites with high potential for transmission had low actual transmission (i.e., false positives far exceeded false negatives). Socio-ecological factors such as vector control effort might explain these false positives. For example, many countries in Latin America and the Caribbean economically depend on tourism, and are likely to invest heavily in preventing outbreaks. We therefore expect these countries to have lower transmission than predicted by the model. Indeed, while the temperature-dependent model predicted maximum incidence well for data from countries with low to medium dependence on tourism, countries with the heaviest reliance on tourism had no correlation between expected and observed transmission (10^{th}, 50^{th}, and 90^{th} percentile, respectively, in proportion of GDP that comes from tourism; Fig. 2). In sum, mean temperature alone predicts where transmission and large epidemics can and cannot occur, while factors correlated with economic reliance on tourism explain lower than expected transmission in some sites with highly suitable temperatures.

The validated model predicts where transmission is not excluded (a conservative estimate of transmission risk). Considering the number of months per year at which mean temperatures do not prevent transmission (i.e., $R_0 > 0$; since our model is relativized, we cannot estimate where absolute $R_0 > 1$), large areas of tropical and subtropical regions, including Puerto Rico and parts of Florida and Texas, are currently suitable year-round or seasonally (Fig. 3). These regions are fundamentally at risk for DENV, CHIKV, ZIKV, and other *Aedes* arbovirus transmission during a substantial part of the year (Fig. 3). On the other hand, many temperate regions experience temperatures suitable for transmission 3 months or less per year (Fig. 3), and the virus incubation periods in humans and mosquitoes restrict the transmission window even further. Temperature thus limits the potential for the viruses to generate extensive epidemics in temperate areas even

where the vectors are present. Moreover, many temperate regions with seasonally suitable temperatures currently lack *Ae. aegypti* and *Ae. albopictus* mosquitoes, making vector transmission impossible (Fig. S7).

Discussion

Predicting the geographic and seasonal potential for transmission of Zika is particularly important in light of the upcoming Olympic games in Brazil in August 2016. Over the last 10 years, the mean temperature in Rio de Janeiro in August has been 22.2°C, which is at the low end of the predicted suitable range for transmission (Fig. 1, lines). Observed transmission rates of ZIKV, DENV, and CHIKV have been low at this temperature (Fig. 1, points). The temperature suitability for transmission during the Olympics is relatively low compared with the Brazilian summer (e.g., during Carnival in February, when the 10-year mean temperature is 27.6°C, nearly optimal for transmission). Moreover, transmission risk during the 2016 Olympics also depends on mosquito abundance and biting rate, control efforts, infrastructure, and the number of susceptible visitors. Together, low temperature suitability, vector control efforts, and infrastructure improvements may limit ZIKV transmission risk during the Rio Olympics. The possibility of new epidemics arising from cases exported from the 2016 Olympics is an additional risk. Regions with longer transmission seasons (e.g., >3 months) could have suitable temperatures beyond the August 21, 2016 closing ceremony (e.g., the Southeastern US), but much of the temperate northern hemisphere is expected to have at most a short transmission window following the Olympics (Fig. S7).

The socio-ecological conditions that enabled CHIKV, ZIKV, and DENV to become the three most important emerging vector-borne diseases in the Americas make further *Aedes*-transmitted virus emergence likely (e.g., Rift Valley fever virus, yellow fever virus, Uganda S

185 virus, Ross River Virus). Efforts to extrapolate and to map temperature suitability (Fig. 3) will be
186 critical for improving management of both ongoing and future emerging epidemics. Whereas
187 statistical models are well suited for accurate interpolation from existing distribution ranges (5),
188 mechanistic models are useful for extrapolating beyond current distributions. These mechanistic
189 models are especially important for effects of temperature because thermal responses are well
190 known to be nonlinear (Figs. S1-S2) and because thermal responses of multiple traits must be
191 integrated to accurately predict temperature suitability for transmission and thus to extrapolate
192 beyond the current distribution of the viruses. Strikingly, we show that our model based just on
193 temperature is able to bound human incidence for DENV, CHIKV, and ZIKV (Fig. 1). Socio-
194 ecological factors such as vector control effort and infrastructure (for which the proportion of
195 GDP in tourism might be a proxy) explain additional variation in transmission in suitable areas
196 (Fig. 2). Accurately estimating temperature-driven transmission risk in both highly suitable and
197 marginal regions is critical for predicting and responding to future outbreaks of these and other
198 *Aedes*-transmitted viruses.

199 **Materials and Methods**

200 Temperature-sensitive R_0 models

201 We constructed temperature-dependent models of transmission using a previously
202 developed R_0 framework. We modeled transmission rate as the basic reproduction rate, R_0—the
203 number of secondary infections that would originate from a single infected individual introduced
204 to a fully susceptible population. In previous work on malaria, we adapted a commonly used
205 expression for R_0 for vector transmission to include the temperature-sensitive traits that drive
206 mosquito population density (11):

$$R_0(T) = \left(\frac{a(T)^2 \, b(T) \, c(T) \, e^{-\mu(T)/PDR(T)} \, EFD(T) \, p_{EA}(T) \, MDR(T)}{N \, r \, \mu(T)^3} \right)^{1/2} \quad (1)$$

Here, (T) indicates that the trait is a function of temperature, T; a is the per-mosquito biting rate, b is the proportion of infectious bites that infect susceptible humans, c is the proportion of bites on infected humans that infect previously uninfected mosquitoes (i.e., $b*c$ = vector competence), μ is the adult mosquito mortality rate (lifespan, $lf = 1/\mu$), PDR is the parasite development rate (i.e., the inverse of the extrinsic incubation period, the time required between a mosquito biting an infected host and becoming infectious), EFD is the number of eggs produced per female mosquito per day, p_{EA} is the mosquito egg-to-adult survival probability, MDR is the mosquito immature development rate (i.e., the inverse of the egg-to-adult development time), N is the density of humans, and r is the human recovery rate. For each temperature-sensitive trait in each mosquito species, we fit either symmetric (Quadratic, $c(T - T_0)(T - T_m)$) or asymmetric (Brière, $cT(T - T_0)(T_m - T)^{1/2}$) unimodal thermal response models to the available empirical data (29). In both functions, T_0 and T_m are respectively the minimum and maximum temperature for transmission, and c is a rate constant. We normalized the R_0 equation to take values between 0-1 because absolute values of R_0 depend on additional factors not captured in our model. Therefore, $R_0 > 0$ is an absolute threshold for whether or not transmission is possible, but the model does not predict when transmission is stable (i.e., absolute $R_0 > 1$).

We fit the trait thermal responses in equation (1) based on an exhaustive search of published laboratory studies that fulfilled the criterion of measuring a trait at three or more constant temperatures, ideally capturing both the rise and the fall of each unimodal curve (Tables S1-S2). Constant-temperature laboratory conditions are required to isolate the direct effect of temperature from confounding factors in the field and to provide a baseline for estimating the effects of temperature variation through rate summation (30). We attempted to obtain raw data

from each study, but if they were not available we collected data by hand from tables or digitized data from figures using WebPlotDigitizer (31). We obtained raw data from Delatte (18) and Alto (20) for the *Ae. albopictus* egg-to-adult survival probability (*pEA*), mosquito development rate (MDR), gonotrophic cycle duration (GCD) and total fecundity (TFD) (Table S2). Data did not meet the inclusion criterion for CHIKV or ZIKV extrinsic incubation period (EIP) in either *Ae. albopictus* or *Ae. aegypti*. Instead, we used DENV EIP data, combined with sensitivity analyses.

Following Johnson *et al.* (32), we fit a thermal response for each trait using Bayesian models. We first fit Bayesian models for each trait thermal response using uninformative priors ($T_0 \sim$ Uniform (0, 24), $T_m \sim$ Uniform (25, 45), $c \sim$ Gamma (1, 10) for Brière and $c \sim$ Gamma (1, 1) for Quadratic fits) chosen to restrict each parameter to its biologically realistic range (i.e., $T_0 < T_m$ and we assumed that temperatures below 0°C and above 45°C were lethal). Any negative values for all thermal response functions were truncated at zero, and thermal responses for probabilities (p_{EA}, b, and c) were also truncated at one. We modeled the observed data as arising from a normal distribution with the mean predicted by the thermal response function calculated at the observed temperature, and the precision τ, ($\tau = 1/\sigma$), distributed as $\tau \sim$ Gamma (0.0001, 00001). We fit the models using Markov Chain Monte Carlo (MCMC) sampling in JAGS, using the R (33) package *rjags* (34). For each thermal response, we ran five MCMC chains with a 5000-step burn-in and saved the subsequent 5000 steps. We thinned the posterior samples by saving every fifth sample and used the samples to calculate R_0 from 15-35°C, producing a posterior distribution of R_0 versus temperature. We summarized the relationship between temperature and each trait or overall R_0 by calculating the mean and 95% highest posterior density interval (HPD interval; a type of credible interval that includes the smallest continuous

252 range containing 95% of the probability, as implemented in the *coda* package (35)) for each
253 curve across temperatures.

254 We fit a second set of models for each mosquito species that used informative priors, for
255 two purposes: 1) to reduce uncertainty in R_0 versus temperature and in the trait thermal
256 responses, and 2) to ensure that our results were not overly dependent on the particular set of
257 data available. In these models, we used Gamma-distributed priors for each parameter T_0, T_m, c,
258 and τ fit from an additional 'prior' dataset of *Aedes* spp. trait data that did not meet the inclusion
259 criteria for the primary dataset (Table S3). We found that these initial informative priors could
260 have an overly strong influence on the posteriors, in some cases drawing the posterior
261 distributions well away from the primary dataset, which was better controlled and met the
262 inclusion criteria. We accounted for our lower confidence in this data set by increasing the
263 variance in the informative priors, by multiplying all hyperparameters (i.e., the parameters of the
264 Gamma distributions of priors for T_0, T_m, and c) by a constant k to produce a distribution with the
265 same mean but 1/k times larger variance. We chose the value of k based on our relative
266 confidence in the prior versus main data. Thus we chose k = 0.5 for *b, c,* and *PDR* and k = 0.01
267 for *lf*. This is the main model presented in the text. It is comparable to some but not all previous
268 mechanistic models for *Ae. aegypti* and *Ae. albopictus* transmission (Fig. S8). Results of our
269 main model, fit with informative priors, did not vary substantially from the model fit with
270 uninformative priors (Figs. S9-S10).

271 Effects of humidity on dengue R_0

272 Like temperature, humidity is expected to affect vector transmission via its effects on
273 mosquito populations. Specifically, we expected humidity to affect egg-to-adult survival and
274 adult survival. Using the methods described above, we extracted laboratory data on these traits at

constant humidity in the laboratory. We searched for *Aedes* spp. survival probability data across temperature and humidity. We obtained data on *Aedes aegypti* egg hatching probability (36) and *Anopheles gambiae* lifespan (37), which we used in absence of *Aedes* spp. because they have a similar (tropical, anthrophilic) life history. We used linear regression to estimate the relationship between these traits and relative humidity (%), plugged them into the $R_0(T)$ equation (assuming the probability of egg hatching and egg-to-adult survival have the same relationship with humidity), and plotted R_0 versus temperature across a range of relative humidity values (Fig. S3). For the dataset that included variation in temperature and humidity independently, there was no interaction between the unimodal temperature response and the linear humidity response (i.e., humidity did not affect the relationship between lifespan and temperature) (37). The resulting relationship between R_0 and relative humidity was exponential.

Incorporating daily temperature variation in transmission models

Because organisms do not typically experience constant temperature environments in the field, we incorporated the effects of temperature variation on transmission by calculating a daily average R_0 assuming a daily temperature range of 8°C, across a range of mean temperatures. This range is consistent with daily temperature variation in tropical and subtropical environments but lower than in most temperate environments. At each mean temperature, we used a Parton-Logan model to generate hourly temperatures and calculate each temperature-sensitive trait on an hourly basis (38). We assumed an irreversible high-temperature threshold above which mosquitoes die and transmission is impossible (39, 40). We set this threshold based on hourly temperatures exceeding the critical thermal maximum (T_m in Tables S1-S2) for egg-to-adult survival or adult longevity by any amount for five hours or by 3°C for one hour. We averaged each trait over 24 hours to obtain a daily average trait value, which we used to calculate relative

298 R_0 across a range of mean temperatures. We used this model to predict human relative incidence
299 (Fig. 1).

300 DENV, CHIKV, and ZIKV incidence data

301 To validate our model, we plotted the rate of new human cases of DENV, CHIKV, and
302 ZIKV against mean temperature during the transmission window. We downloaded and manually
303 entered Pan American Health Organization (PAHO) weekly case reports for DENV and CHIKV
304 for all countries in the Americas (North, Central, and South America and the Caribbean Islands)
305 from week 1 of 2014 to week 8 of 2015 for CHIKV and from week 52 of 2013 to week 47 of
306 2015 for DENV (www.paho.org). ZIKV weekly case reports for reporting districts (e.g.,
307 provinces) within Colombia, Mexico, El Salvador, and the US Virgin Islands were available
308 from the CDC Epidemic Prediction Initiative (https://github.com/cdcepi/) from November 28,
309 2015 to March 1, 2016. Additional serotype-specific DENV case data (matched with temperature
310 and other covariates) were available from the Dengue Forecasting Challenge
311 (www.dengueforecasting.noaa.gov/) for Iquitos, Peru from 2000-2013 and for San Juan, Puerto
312 Rico from 1990-2013. We manually selected separate epidemics of different DENV serotypes by
313 examining the weekly incidence data plotted over time.

314 Incidence of human cases has a nonlinear relationship with transmission potential (R_0 or
315 the number of infectious mosquitoes per person). During the rising phase of an epidemic, new
316 cases arise more quickly as the epidemic gets larger, while during the declining phase, the
317 exhaustion of the susceptible population leads to declines in transmission (41). We controlled for
318 this nonlinearity in two ways. First, we calculated relative incidence as the number of new cases
319 divided by the total number of cases to date. Second, we removed the declining portion of each

epidemic from analyses. We did this by discarding all data following the first week that relative incidence was less than the average over the preceding ten weeks.

Temperature data collection

We matched the PAHO DENV and CHIKV incidence data with temperature using daily temperature data from METAR stations in each country, averaged at the country level by epidemic week. We assumed a two-week lag between temperature and incidence (i.e., mean temperature for the week that is two weeks prior to each case report). METAR stations are internationally standardized weather reporting stations that report hourly temperature and precipitation measures. Outlier weather stations were excluded if they reported a daily maximum temperature below 5°C or a daily minimum temperature below 40°C during the study period, extremes that would certainly eliminate the potential for transmission in a local area. Because case data are reported at the country level, we needed a collection of weather stations in each country that accurately represent weather conditions in the areas where transmission occurs, excluding extreme areas where transmission is unlikely. For the study period of October 1, 2013 through January 10, 2016, we downloaded daily temperature data for each station from Weather Underground using the *weatherData* package in R (42). This totaled 523 stations for 49 countries. We removed all data from Chile because it spans so much latitude and the terrain is so diverse that its country-level mean is unlikely to be very representative of the temperature where an outbreak occurred. For ZIKV, we manually selected weather stations in or near each reporting area (department within country). El Salvador and the US Virgin Islands each had only two weather stations, which we used for all reporting locations within those countries.

Validation analyses with human incidence versus temperature datasets

342 To validate our model predictions for transmission, we plotted each time point for
343 relative incidence against mean temperature from two weeks earlier for DENV, CHIKV, and
344 ZIKV. Within a set of reports with similar temperatures, we expected the sites with the highest
345 relative incidence to represent those where transmission is least limited by vector control and
346 other socio-ecological factors. We selected these maxima within a set of temperature bins for
347 each incidence dataset (PAHO DENV, CHIKV, and ZIKV). To determine the size of each bin,
348 we took the subset of each dataset with non-zero relative incidence and created bins of equal size
349 for a total of 20 bins. These maxima are highlighted with filled circles in Fig. 1.

350 We were then interested whether relative incidence maxima would be highest at the most
351 suitable temperatures predicted by the model (~26-29°C), and lower at temperatures predicted to
352 be less suitable. To examine this relationship, we plotted predicted transmission rate against
353 observed relative incidence for the maximum points only, using the best-fit prediction from
354 either the *Ae. aegypti* or the *Ae. albopictus* R_0 model because the mosquito vector responsible for
355 transmission often is not known (5).

356 Even for the maximum relative incidence at each temperature, we expect some variation
357 to be explained by socio-ecological conditions beyond temperature. In particular, countries that
358 rely heavily on tourism should be highly motivated to prevent epidemics, and thus the proportion
359 of GDP in tourism might be a good proxy for vector control effort and infrastructure that
360 prevents human-mosquito contact (air conditioning and window screens). Based on this
361 motivation, we conducted a linear mixed-effects model with observed maximum incidence data
362 (from the 20 bins for each virus) as the Gaussian response variable, country as a random effect,
363 and virus species, predicted R_0 from the mechanistic model, log of percent of GDP in tourism,
364 and a predicted R_0-by-GDP interaction as predictors. We plotted the expected versus observed

365 transmission relationship based on whether the outbreak origin was in the 10^{th}, 50^{th}, or 90^{th}
366 percentile of countries in percent of GDP in tourism, using the R package *visreg* (43). Each point
367 in this partial residual plot (Fig. 2) appears only once in the panel to which it is closest. However,
368 the least squares estimates from the mixed model are not equivalent to drawing a line through the
369 partial residuals because they draw on the pooled data that are shown in separate panels (43).

370 Mapping temperature suitability for transmission

371 Using our validated model, we were interested in where the temperature was suitable for
372 *Ae. aegypti* and/or *Ae. albopictus* transmission for some or all of the year to predict the potential
373 geographic range of outbreaks in the Americas. We visualized the minimum, median, and
374 maximum extent of transmission based on probability of occurrence thresholds from the R_0
375 models for both mosquitoes. We calculated the number of consecutive months in which the
376 posterior probability of $R_0 > 0$ exceeds a threshold of 0.025, 0.5, or 0.975 for both mosquito
377 species, representing the maximum, median, and minimum likely ranges, respectively. This
378 analysis indicates the predicted seasonality of temperature suitability for transmission
379 geographically, but does not indicate its magnitude. To generate the maps, we cropped monthly
380 mean temperature rasters for all twelve months (Worldclim; www.worldclim.org/) to the
381 Americas (*R*, *raster* package, *crop* function) and assigned cells values of 1 or 0 depending on
382 whether the probability that $R_0 > 0$ exceeded the threshold at the temperatures in those cells
383 (Table S3). We then synthesized the monthly grids into a single raster that reflected the
384 maximum number of consecutive months where cell values equaled 1. For plotting, rasters were
385 overlaid on a global country polygon map (*rworldmap* package (44)). We repeated this process
386 for each combination of mosquito species and posterior probability thresholds.

387

Acknowledgments

EAM, MBT, VS, SJR, LRJ, ASI, JRR, MS, JC, and DPW were supported by the National Science Foundation (DEB-1518681). J.R.R. was supported by the NSF (EF-1241889), National Institutes of Health (R01GM109499 and R01TW010286-01), US Department of Agriculture (2009-35102-0543) and US Environmental Protection Agency (CAREER 83518801). EAM and CCM were supported by the NSF (DEB-1640780). Barry Alto, Krijn Paaijmans, Francis Ezeakacha, and Helene Delatte kindly provided raw data used in the analyses. We gratefully acknowledge the Centers for Disease Control and Prevention Epidemic Predictions Initiative (CDC EPI) for collating and sharing the Zika incidence data on GitHub (https://zenodo.org/record/48946#.Vz-EM2bb8ys). The authors declare no competing interests.

References:

1. Brady OJ, et al. (2012) Refining the global spatial limits of dengue virus transmission by evidence-based consensus. *PLOS Negl Trop Dis* 6(8):e1760.

2. Bhatt S, et al. (2013) The global distribution and burden of dengue. *Nature* 496(7446):504–507.

3. Rasmussen SA, Jamieson DJ, Honein MA, Petersen LR (2016) Zika virus and birth defects — reviewing the evidence for causality. *N Engl J Med* 374:1981–1987.

4. Scott TW, Takken W (2012) Feeding strategies of anthropophilic mosquitoes result in increased risk of pathogen transmission. *Trends Parasitol* 28(3):114–121.

5. Messina JP, et al. (2016) Mapping global environmental suitability for Zika virus. *eLife* 5:e15272.

6. Magori K, et al. (2009) Skeeter Buster: A stochastic, spatially explicit modeling tool for studying *Aedes aegypti* population replacement and population suppression strategies. *PLOS Negl Trop Dis* 3(9):e508.

7. Johansson MA, Powers AM, Pesik N, Cohen NJ, Staples JE (2014) Nowcasting the spread of chikungunya virus in the Americas. *PLoS ONE* 9(8):e104915.

8. Perkins TA, Metcalf CJE, Grenfell BT, Tatem AJ (2015) Estimating drivers of autochthonous transmission of chikungunya virus in its invasion of the Americas. *PLoS Curr* 7. doi:10.1371/currents.outbreaks.a4c7b6ac10e0420b1788c9767946d1fc.

421 9. Morin CW, Monaghan AJ, Hayden MH, Barrera R, Ernst K (2015) Meteorologically driven
422 simulations of dengue epidemics in San Juan, PR. *PLoS Negl Trop Dis* 9(8):e0004002.

423 10. Dell AI, Pawar S, Savage VM (2011) Systematic variation in the temperature dependence
424 of physiological and ecological traits. *Proc Natl Acad Sci* 108(26):10591–10596.

425 11. Mordecai EA, et al. (2013) Optimal temperature for malaria transmission is dramatically
426 lower than previously predicted. *Ecol Lett* 16:22–30.

427 12. Focks DA, Haile DG, Daniels E, Mount GA (1993) Dynamic life table model for *Aedes*
428 *aegypti* (Diptera: Culicidae): analysis of the literature and model development. *J Med*
429 *Entomol* 30(6):1003–1017.

430 13. Yang HM, Macoris MLG, Galvani KC, Andrighetti MTM, Wanderley DMV (2009)
431 Assessing the effects of temperature on the population of *Aedes aegypti*, the vector of
432 dengue. *Epidemiol Infect* 137(8):1188–1202.

433 14. Rueda L, Patel K, Axtell R, Stinner R (1990) Temperature-dependent development and
434 survival rates of *Culex quinquefasciatus* and *Aedes aegypti* (Diptera: Culicidae). *J Med*
435 *Entomol* 27(5):892–898.

436 15. Tun-Lin W, Burkot TR, Kay BH (2000) Effects of temperature and larval diet on
437 development rates and survival of the dengue vector *Aedes aegypti* in north Queensland,
438 Australia. *Med Vet Entomol* 14(1):31–37.

439 16. Kamimura K, et al. (2002) Effect of temperature on the development of *Aedes aegypti* and
440 *Aedes albopictus*. *Med Entomol Zool* 53(1):53–58.

17. Eisen L, et al. (2014) The impact of temperature on the bionomics of *Aedes (Stegomyia) aegypti*, with special reference to the cool geographic range margins. *J Med Entomol* 51(3):496–516.

18. Delatte H, Gimonneau G, Triboire A, Fontenille D (2009) Influence of temperature on immature development, survival, longevity, fecundity, and gonotrophic cycles of *Aedes albopictus*, vector of chikungunya and dengue in the Indian Ocean. *J Med Entomol* 46(1):33–41.

19. Muturi EJ, Lampman R, Costanzo K, Alto BW (2011) Effect of temperature and insecticide stress on life-history traits of *Culex restuans* and *Aedes albopictus* (Diptera: Culicidae). *J Med Entomol* 48(2):243–250.

20. Alto BW, Juliano SA (2001) Temperature effects on the dynamics of *Aedes albopictus* (Diptera: Culicidae) populations in the laboratory. *J Med Entomol* 38(4):548–556.

21. Westbrook CJ, Reiskind MH, Pesko KN, Greene KE, Lounibos LP (2010) Larval environmental temperature and the susceptibility of *Aedes albopictus* Skuse (Diptera: Culicidae) to chikungunya virus. *Vector-Borne Zoonotic Dis* 10(3):241–247.

22. Briegel H, Timmermann SE (2001) *Aedes albopictus* (Diptera: Culicidae): Physiological aspects of development and reproduction. *J Med Entomol* 38(4):566–571.

23. Calado DC, Navarro-Silva MA (2002) Influência da temperatura sobre a longevidade, fecundidade e atividade hematofágica de *Aedes (Stegomyia) albopictus* Skuse, 1894 (Diptera, Culicidae) sob condições de laboratório. *Rev Bras Entomol* 46(1):93–98.

461 24. Xiao F-Z, et al. (2014) The effect of temperature on the extrinsic incubation period and
462 infection rate of dengue virus serotype 2 infection in *Aedes albopictus*. *Arch Virol*
463 159(11):3053–3057.

464 25. Watts DM, Burke DS, Harrison BA, Whitmire RE, Nisalak A (1987) Effect of temperature
465 on the vector efficiency of *Aedes aegypti* for dengue 2 virus. *Am J Trop Med Hyg*
466 36(1):143–152.

467 26. McLean DM, et al. (1974) Vector capability of *Aedes aegypti* mosquitoes for California
468 encephalitis and dengue viruses at various temperatures. *Can J Microbiol* 20(2):255–262.

469 27. Carrington LB, Armijos MV, Lambrechts L, Scott TW (2013) Fluctuations at a low mean
470 temperature accelerate dengue virus transmission by *Aedes aegypti*. *PLoS Negl Trop Dis*
471 7(4):e2190.

472 28. Alto BW, Bettinardi D (2013) Temperature and dengue virus infection in mosquitoes:
473 independent effects on the immature and adult stages. *Am J Trop Med Hyg* 88(3):497–505.

474 29. Briere J-F, Pracros P, Le Roux A-Y, Pierre J-S (1999) A novel rate model of temperature-
475 dependent development for arthropods. *Environ Entomol* 28(1):22–29.

476 30. Lambrechts L, et al. (2011) Impact of daily temperature fluctuations on dengue virus
477 transmission by Aedes aegypti. *Proc Natl Acad Sci* 108(18):7460–7465.

478 31. Rohatgi A (2015) *WebPlotDigitizer* Available at: http://arohatgi.info/WebPlotDigitizer.

479 32. Johnson LR, et al. (2015) Understanding uncertainty in temperature effects on vector-borne
480 disease: a Bayesian approach. *Ecology* 96(1):203–213.

481 33. R Development Core Team (2014) *R: A Language and Environment for Statistical*
482 *Computing* (R Foundation for Statistical Computing, Vienna, Austria) Available at:
483 http://www.R-project.org.

484 34. Plummer M (2016) *rjags: Bayesian Graphical Models using MCMC* Available at:
485 http://CRAN.R-project.org/package=rjags.

486 35. Plummer M, Best N, Cowles K, Vines K (2006) *CODA: Convergence Diagnosis and*
487 *Output Analysis for MCMC*.

488 36. Dickerson CZ (2007) The effects of temperature and humidity on the eggs of *Aedes aegypti*
489 (L.) and *Aedes albopictus* (skuse) in Texas. Doctoral (Texas A & M University, College
490 Station, Texas).

491 37. Bayoh MN (2001) Studies on the development and survival of *Anopheles gambiae* sensu
492 stricto at various temperatures and relative humidities. Doctoral (Durham University).
493 Available at: http://etheses.dur.ac.uk/4952/ [Accessed October 15, 2014].

494 38. Parton WJ, Logan JA (1981) A model for diurnal variation in soil and air temperature.
495 *Agric Meteorol* 23:205–216.

496 39. Paaijmans KP, et al. (2013) Temperature variation makes ectotherms more sensitive to
497 climate change. *Glob Change Biol* 19(8):2373–2380.

498 40. Vasseur DA, et al. (2014) Increased temperature variation poses a greater risk to species
499 than climate warming. *Proc R Soc Lond B Biol Sci* 281(1779):20132612.

500 41. Keeling MJ, Rohani P (2008) *Modeling Infectious Diseases in Humans and Animals*
501 (Princeton University Press).

502 42. Narasimhan R (2014) *weatherData: Get Weather Data from the Web* Available at:
503 https://cran.r-project.org/web/packages/weatherData/index.html [Accessed May 25, 2016].

504 43. Breheny P, Burchett W (2016) *visreg: Visualization of Regression Models* Available at:
505 https://cran.r-project.org/web/packages/visreg/index.html [Accessed June 8, 2016].

506 44. South A (2016) *rworldmap: Mapping Global Data* Available at: https://cran.r-
507 project.org/web/packages/rworldmap/index.html [Accessed June 10, 2016].

508 45. Wesolowski A, et al. (2015) Impact of human mobility on the emergence of dengue
509 epidemics in Pakistan. *Proc Natl Acad Sci*:201504964.

510 46. Liu-Helmersson J, Stenlund H, Wilder-Smith A, Rocklöv J (2014) Vectorial capacity of
511 *Aedes aegypti*: Effects of temperature and implications for global dengue epidemic
512 potential. *PLoS ONE* 9(3):e89783.

513 47. Focks DA, Haile DG, Daniels E, Mount GA (1993) Dynamic life table model for *Aedes*
514 *aegypti* (Diptera: Culicidae): analysis of the literature and model development. *J Med*
515 *Entomol* 30(6):1003–1017.

516 48. Ezeakacha N (2015) Environmental impacts and carry-over effects in complex life cycles:
517 the role of different life history stages. *Dissertation*. Available at:
518 http://aquila.usm.edu/dissertations/190.

519 49. Beserra EB, Fernandes CRM, Silva SA de O, Silva LA da, Santos JW dos (2009) Efeitos da
520 temperatura no ciclo de vida, exigências térmicas e estimativas do número de gerações
521 anuais de *Aedes aegypti* (Diptera, Culicidae). *Iheringia Sér Zool*. Available at:
522 http://agris.fao.org/agris-search/search.do?recordID=XS2010500501 [Accessed September
523 10, 2015].

524 50. Joshi DS (1996) Effect of fluctuating and constant temperatures on development, adult
525 longevity and fecundity in the mosquito *Aedes krombeini*. *J Therm Biol* 21(3):151–154.

526 51. Westbrook CJ (2010) Larval ecology and adult vector competence of invasive mosquitoes
527 *Aedes albopictus* and *Aedes aegypti* for Chikungunya virus. Dissertation (University of
528 Florida). Available at: http://etd.fcla.edu/UF/UFE0041830/westbrook_c.pdf [Accessed
529 October 23, 2013].

530 52. Wiwatanaratanabutr S, Kittayapong P (2006) Effects of temephos and temperature on
531 Wolbachia load and life history traits of *Aedes albopictus*. *Med Vet Entomol* 20(3):300–
532 307.

533 53. Teng H-J, Apperson CS (2000) Development and Survival of Immature *Aedes albopictus*
534 and *Aedes triseriatus* (Diptera: Culicidae) in the Laboratory: Effects of Density, Food, and
535 Competition on Response to Temperature. *J Med Entomol* 37(1):40–52.

536 54. Tun-Lin W, Burkot T, Kay B (2000) Effects of temperature and larval diet on development
537 rates and survival of the dengue vector *Aedes aegypti* in north Queensland, Australia. *Med*
538 *Vet Entomol* 14(1):31–37.

539 55. Jalil M (1972) Effect of temperature on larval growth of *Aedes triseriatus*. *J Econ Entomol*
540 65(2):625–626.

541 56. Calado DC, Silva MAN da (2002) Avaliação da influência da temperatura sobre o
542 desenvolvimento de *Aedes albopictus*. *Rev Saúde Pública* 36(2):173–179.

543 57. Couret J, Dotson E, Benedict MQ (2014) Temperature, larval diet, and density effects on
544 development rate and survival of *Aedes aegypti* (Diptera: Culicidae). *PLoS ONE*
545 9(2):e87468.

546 58. Davis NC (1932) The effect of various temperatures in modifying the extrinsic incubation
547 period of the yellow fever virus in *Aedes aegypti*. *Am J Epidemiol* 16(1):163–176.

548 59. Focks DA, Daniels E, Haile DG, Keesling JE (1995) A simulation model of the
549 epidemiology of urban dengue fever: literature analysis, model development, preliminary
550 validation, and samples of simulation results. *Am J Trop Med Hyg* 53(5):489–506.

551 60. McLean DM, Miller MA, Grass PN (1975) Dengue virus transmission by mosquitoes
552 incubated at low temperatures. *Mosq News*. Available at: http://agris.fao.org/agris-
553 search/search.do?recordID=US19760088008 [Accessed August 26, 2015].

554 61. Reisen WK, Fang Y, Martinez VM (2006) Effects of temperature on the transmission of
555 West Nile virus by *Culex tarsalis* (Diptera: Culicidae). *J Med Entomol* 43(2):309–317.

556

557

Figure Captions

Fig. 1. Relative R_0 (assuming an 8°C daily temperature range) versus mean temperature (°C) for *Ae. albopictus* (light blue line) and *Ae. aegypti* (dark blue line). For validation, weekly relative incidence of DENV (dark blue points, N = 1,195), CHIKV (gray points, N = 1,642), and ZIKV (red points, N = 10,741) are plotted against the mean temperature two weeks prior to each reporting date. Filled circles represent the maximum relative incidence within each temperature bin for each virus (20 bins per virus). Both R_0 curves and the relative incidence of the three viruses are each normalized to a 0-1 scale for ease of comparison and visualization.

Fig. 2. A partial residual plot showing the relationship between the predicted transmission rate (relative R_0) from the mechanistic model and the observed maximum relative incidence (rate of new cases divided by cumulative cases; filled circles in Fig. 1, N = 59) for dengue, chikungunya, and Zika as a function of the proportion of a country's gross domestic product (GDP) that comes from tourism. The percent of GDP from tourism is used as a proxy for vector control effort and infrastructure that prevents mosquito contacts (air conditioning and window screens). Lines and 95% confidence intervals are based on the entire dataset, even though the data are plotted in three discrete percentile groups (see Materials and Methods and Supplemental Results for details). Predicted R_0 from the mechanistic model ($X^2 = 10.26$, $df = 1$, $p = 0.001$) and its interaction with the log of percent of GDP in tourism ($X^2 = 4.14$, $df = 1$, $p = 0.042$) significantly predicted the observed maximum relative incidence.

Fig. 3. Map of predicted temperature suitability for virus transmission by *Ae. albopictus* and *Ae. aegypti*. Color indicates the consecutive months in which temperature is permissive for

581 transmission (predicted $R_0 > 0$) for *Aedes* spp. transmission. Red, minimum likely range (>
582 97.5% probability that $R_0 > 0$), purple, median likely range (> 50% probability that $R_0 > 0$), teal,
583 maximum likely range (> 2.5% probability that $R_0 > 0$). Model suitability predictions combine
584 temperature mean and 8°C daily variation and are informed by laboratory data (Figs. S1-S2) and
585 validated against field data (Figs. 1-2).
586

587 Figure 1

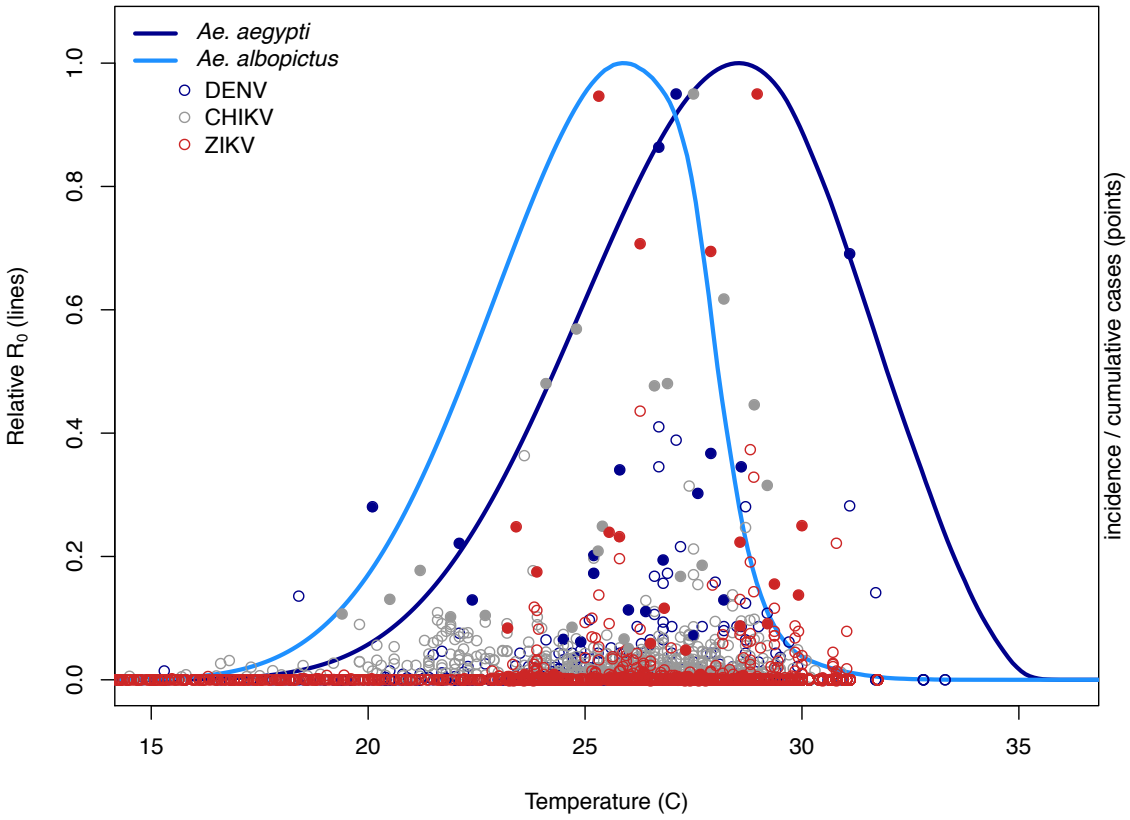

588

589 Figure 2

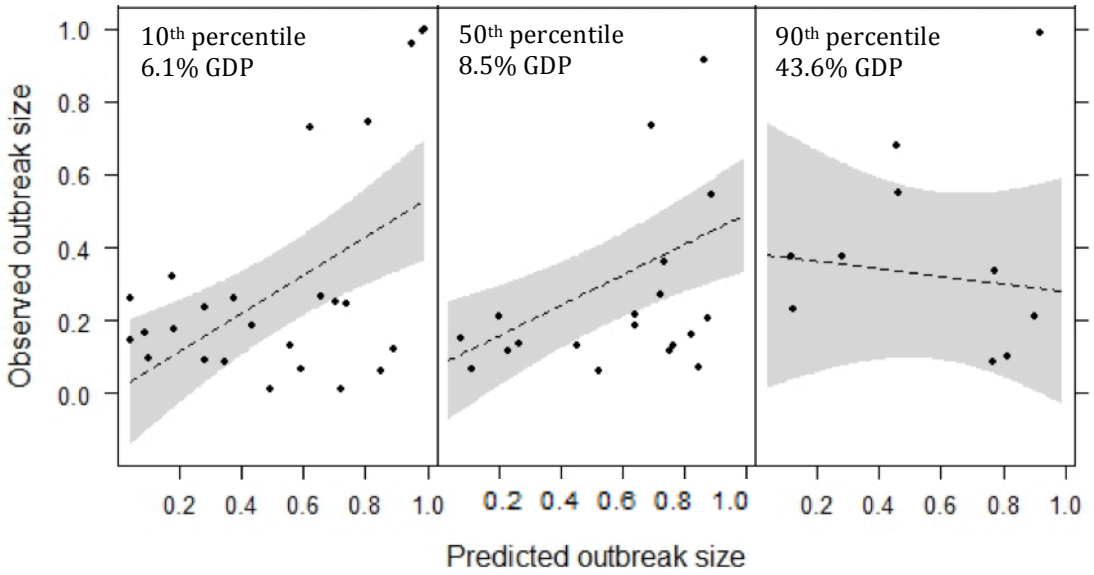

590

591

592 Figure 3

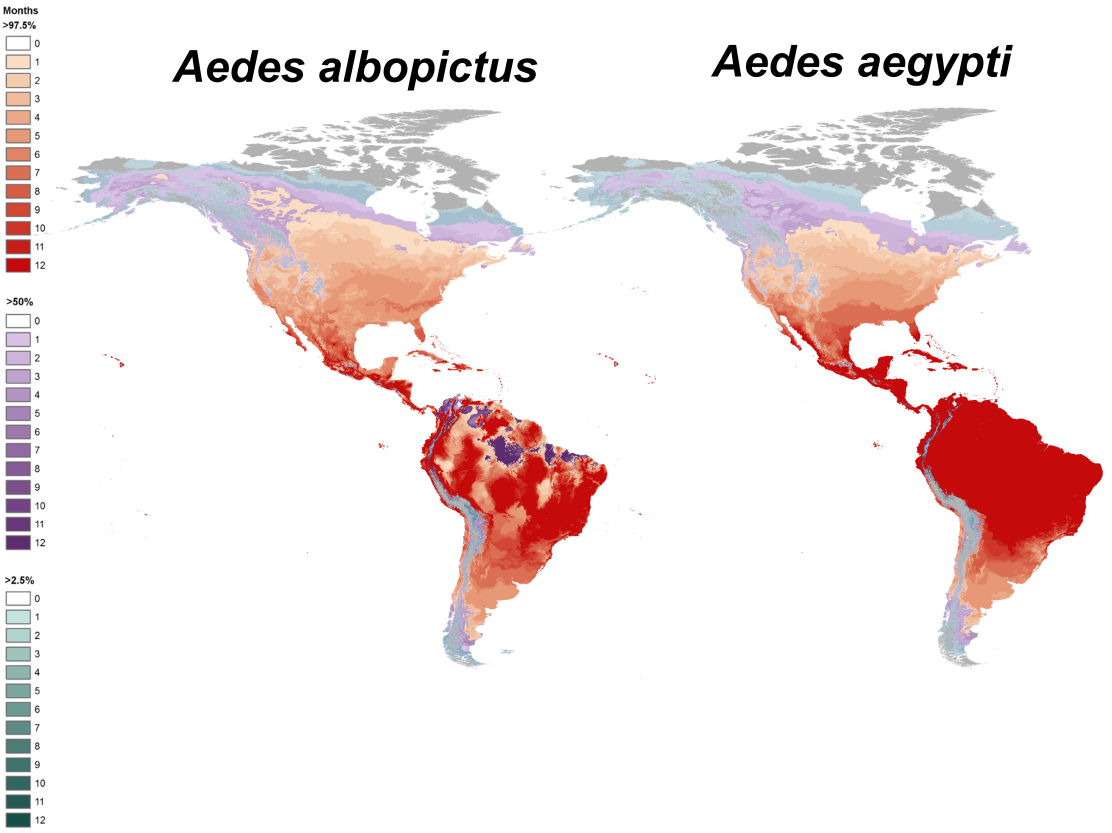

593

594